



Phytochemical-assisted Synthesis of Titania Nanoparticles using *Cassia alata* Leaf Extract as Photocatalyst in the Photodegradation of Bisphenol A

Nurfatin Azira Karyadi, Sheela Chandren*, Norazah Basar

Department of Chemistry, Faculty of Science, Universiti Teknologi Malaysia, Johor, Malaysia

*Corresponding author: sheela@utm.my

Abstract

Titania (TiO_2) is one of the most used semiconductor metal oxides in various applications including as photocatalysts, among many others. Numerous methods, such as solvothermal, chemical vapour deposition, and hydrothermal, have been used to synthesize TiO_2 nanoparticles (TiO_2 NPs) but present major drawbacks such as being hard to control, requiring high temperatures and polluting the environment. In this work, the biosynthesis method was chosen to mitigate these drawbacks. First, TiO_2 NPs were biosynthesized using the aqueous leaf extract of *Cassia alata* with different amounts of extract volumes and distilled water as the solvent. Phytochemical testing of the *Cassia alata* leaf extracted from the ultrasound-assisted extraction method gave better results, which can be seen from the higher intensity of colour change, for the presence of phenolic, terpenoid, and flavonoid, compared to those of the maceration and reflux extraction methods. Fourier transform infrared spectroscopy (FTIR) spectra of the extract confirmed the presence of phenolic compounds in *Cassia alata* leaf extract and TiO_2 NPs formation was successfully obtained corresponding to the broad band observed at the region of $400 - 800 \text{ cm}^{-1}$. X-ray diffraction (XRD) patterns showed that the prepared TiO_2 NPs samples were in the anatase phase. Field emission scanning electron microscopy-energy dispersion X-ray (FESEM-EDX) images showed that the NPs were almost spherical in shape with a size range of 15.41 to 22.85 nm. The bandgap energy was calculated using ultraviolet-visible-near-infrared spectroscopy (UV-vis-NIR) and was within the range of anatase TiO_2 . Nitrogen sorption analysis showed that the biosynthesized TiO_2 NPs possess a type V isotherm and H1 type hysteresis loop with a pore size distribution of between 8.0293 and 9.9449 nm and the specific surface area that ranges from 84.4729 to 103.1434 m^2/g . The photocatalytic activity of the synthesized TiO_2 NPs was tested out in the photodegradation of bisphenol A (BPA) under UV light irradiation for 1 h. The sample prepared with 7.5 mL of the leaf extract showed the highest activity, achieving 68.41% of BPA degradation. These results show that the biosynthesis method using *Cassia alata* leaf extract with distilled water as the solvent led to the formation of TiO_2 NPs with good photocatalytic activity.

Keywords: TiO_2 NPs, *Cassia alata*, photocatalyst, photodegradation, Bisphenol A (BPA)

1. Introduction

Photocatalysis is one of the most significant advanced oxidation processes (AOPs) usually used in organic pollutants degradation due to its simplicity, good reproducibility, high efficiency, and ease of handling [1]. Compared to other types of semiconductors, titania (TiO_2) has been given significant attention as it gives a good performance as a photocatalyst under UV light irradiation, is low cost, stable, and non-toxic [2]. TiO_2 is useful in many fields as it is a cost-effective material with superior biological and chemical properties and high oxidising power [3]. In addition, TiO_2 nanoparticles (NPs) have been widely used as the photocatalyst in photocatalytic reactions under mild conditions in both gaseous and aqueous mediums [4]. TiO_2 NPs have also found usage as a self-cleaning agent as it was discovered that TiO_2 , the designated materials of positive electrodes, show self-cleaning functionality and are high in triboelectric nanogenerators power [5].

There are various types of TiO₂ NPs preparation methods that have been studied. For instance, the sol-gel method is usually used in NPs synthesis as it produces better crystalline particles with a high surface area and is smaller in size [6]. Other than that, synthetic methods such as solvothermal, hydrothermal and vapour deposition have also been employed in the preparation of metal oxide NPs with various morphology and size. However, these methods require a high number of chemicals that are hazardous and may have negative impacts on humans and the environment. Additionally, these methods are also high in cost in terms of their preparation and maintenance. Thus, a greener approach is crucial to overcome the limitations of these methods.

In this study, the TiO₂ NPs were biosynthesised by using the extract of *Cassia alata* leaves, with distilled water as the solvent, which is one of the approaches used for green synthesis [6]. Based on previous studies, it is reported that the secondary metabolites consist of terpenoids, flavonoids, saponins, steroids, polyacetylenes amino acids, and alkaloids that are high in bioactivity, less detrimental to mammals and the environment and are effective as reducing and capping agents [7]. For this study, different types of extraction methods have been used to find the most applicable approach before the synthesis of the TiO₂ NPs was done. Different amounts of leaf extract have been used in the synthesis of the TiO₂ NPs. In order to determine the physicochemical properties of the biosynthesised TiO₂ NPs, various instrumentation analyses have been carried out. The photocatalytic activity of the synthesised TiO₂ NPs has been tested out in the photodegradation of Bisphenol A (BPA) under UV light irradiation.

2. Literature review

TiO₂ NPs are polymorphic materials that occur in three different forms of brookite, anatase, and rutile phases [8]. TiO₂ NPs are n-type semiconductors, white in colour with high thermal stability, are excellent in dielectric and optical properties, have high biocompatibility and are non-toxic metals [8]. In addition, TiO₂ semiconductor is also an inexpensive, photo-stable and reusable metal [9]. It is very promising as the TiO₂ NPs have found many uses in various industries, especially in the chemical industry. Owing to the favourable properties of TiO₂ NPs, degradation of contaminants, including dyes and organic pollutants, can be undertaken with relative ease.

TiO₂ is a metal with useful biological and chemical properties and has high oxidising power, in addition to being cost-effective [10]. Due to its benefits, it is gaining more attention compared to other types of semiconductors. TiO₂ has been used in vast applications, including as a photocatalyst, self-cleaning agent, water treatment, lithium-ion batteries, biotechnologies applications and pigment.

The plant extracts used for biosynthesis can be the leaves, roots, fruit peel and fruit [8]. According to [11], using biological ways in synthesizing TiO₂ NPs is more environment-friendly as compared to the conventional methods. In this study, the leaves are used as they contain a high amount of active compounds, including alkaloids, terpenoids, vitamins, phenols, and tannins that are able to act as reducing agents, stabilising and capping purposes [12].

In plant-based biosynthesis of NPs, the biosynthesis of the leaf extract is done together with the sol-gel method due to its simplicity and can be carried out under ambient pressure and temperature [9]. In this work, the leaf extract of *Cassia alata* was added as it contains the biomolecules component that can act as the stabilising and reducing agent in the formation of TiO₂ NPs [13]. Sol-gel synthesis is based on the hydrolysis of a titanium precursor to produce a sol and then a gel, followed by solvent evaporation, where a xerogel is produced [14]. The sol-gel process is the most interesting process and is selected as it undergoes the lower temperature process at <100 °C, which will produce better crystalline particles with a high surface area and smaller sizes of particles [15].

The knowledge of the biosynthesis of TiO₂ using *Cassia alata* for its anti-bacterial and photocatalytic activity warrants a need for expansion as this plant has a wide range of benefits. *Cassia alata* has been used widely in industries, for instance, in phyto-assisted synthesis of zinc oxide nanoparticles for its anti-bacterial activity against *Escherichia coli* [16]. This plant is believed to be able to provide the photocatalyst for the photodegradation of organic pollutants. The synthesis of NPs by using plant extracts such as leaves involves three mechanisms, the first one being the activation phase. During this phase, the metal ions reduction will take place, and the nucleation of reduced metal ions is initiated. The biomolecules take part in the redox reaction [10]. During the growth phase, it involves the

spontaneous aggregation of the small adjacent of nanoparticles that coalesce to form larger size of particles, and the termination phase defines the shape of NPs and marks the last stage of the synthesis of NPs [17].

3. Methodology

The *Cassia alata* leaves were collected from Dusun UTM. The total amount of samples collected was 2.0 kg. The leaf sample (~ 2.0 kg) was washed using tap water to remove impurities. The leaves were left and dried at room temperature under sunlight for 15 days to remove moisture residue before the extraction method was carried out.

3.1. Extraction method

3.1.1 Maceration

The dried leaves sample was ground by using a grinder. The sample amount used was 10 g. Next, 100 mL of distilled water was added to the beaker. Then, the sample was left at room temperature for 2 h. After that, the sample was filtered by using filter paper to separate between residue and filtrate. The filtrate then continues for the phytochemical testing.

3.1.2 Ultrasound-assisted

The dried leaves sample was ground by using a grinder. About 2 g of the sample was sieved and put into the beaker. Next, 20 mL of distilled water was added to it. The sample was stirred and left to run at 20 kHz, at sweep mode for 2 h by using an ultrasound-assisted instrument from FB15057 Fisherbrand. After that, the sample was filtered by using filter paper to separate between residue and filtrate. The filtrate was then used for phytochemical testing.

3.1.3 Heat reflux

The dried leaves sample was ground by using a grinder, where 10 g of the samples was used. Next, 100 mL of distilled water was added to the beaker. Then, the sample was left for reflux extraction for 2 h. After that, the sample was filtered by using filter paper to separate between residue and filtrate. The filtrate was then used for phytochemical testing.

3.2. Phytochemical testing of extracts

3.2.1 Phenolics test

For this test, 5% of ferric chloride was added to 2 mL of the leaf extract; if the results show black colouration, this indicates the presence of phenols.

3.2.2 Flavonoids test

The sample was added to the test tube. Drops of 10% NaOH solution were added to the sample. After the sample mixture turned yellow in colour, the diluted hydrochloric acid (HCl) was added to the mixture drop by drop until the mixture turned colourless. These changes indicate the presence of flavonoids in the sample mixture.

3.2.3 Terpenoids test

Firstly, the sample (~ 5 mL) was added to the test tube. The 2 mL of chloroform was added to the test tube. Last but not least, 3 mL of sulphuric acid was added drop by drop slowly into the mixture. The brown interface indicates the presence of terpenoids in the sample.

3.3. Biosynthesis of TiO_2

Firstly, the titanium(IV) isopropoxide (TTIP) will act as the precursor. The leaf extracts were prepared with distilled water as the medium and prepared in a ratio of 1g/10 mL. Three different amounts of leaf extract were used (2.5, 5.0 and 7.5 mL) by dissolving 4 mL of TTIP with 20 mL of deionised (DI) water (triplicate) under constant stirring for 30 min at 30 °C. Then, *Cassia alata* extracts are gradually added with constant stirring at 50 °C for 4 h. Next, the sample was kept at room condition for 48 h for the ageing process. The resulting colloidal suspension was washed with ethanol, and then the sample was

centrifuged three times at 5,000 rpm for 30 min. After that, the samples were dried at 60 °C for 3 hours and allowed to dry at 95°C for 24 h in an oven before proceeding with the calcination process at 500 °C in a muffle furnace for 5 h.

4. Results and Discussion

4.1 Leaf extraction results

The extraction was done by three types of extraction methods: maceration, reflux, and ultrasound-assisted extraction for 2 h. From the three different extraction methods, as shown in Figure 1, all samples yielded an extract of greenish-brown in colour. The same observation was also obtained by [10], who studied the use of ultrasound-assisted extraction method to obtain the *Cassia alata* leaf extract for further analysis of its constituents in the leaf extract. From these results, the leaf extract obtained was subjected to phytochemical testing and used for the synthesis of TiO₂ NPs.

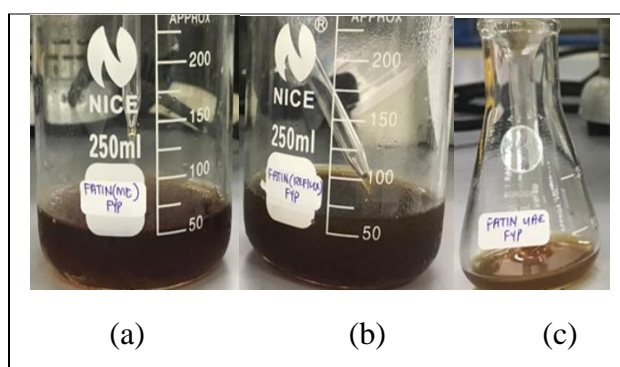


Figure 1. The leaf extract solutions from (a) ultrasound-assisted, (b) maceration and (c) reflux extraction methods

4.2 Phytochemical testing of the extracts

Phytochemical screening tests were done to determine the constituents present in the leaf extract of *Cassia alata*. Based on the phytochemical testing done for all leaf extract samples, the ultrasound-assisted extraction method was chosen due to the higher intensity of colour change obtained for the terpenoids, phenolics, and flavonoids test compared with maceration and heat reflux methods. Table 1 shows the results of the qualitative tests that have been carried out in this work.

Table 1. The result of the phytochemical testing of terpenoids, phenolics and flavonoids.

Constituent	Type of extraction method		
	Maceration extraction	Reflux extraction	Ultrasound-assisted extraction
Terpenoids	+	+	++
Phenolics	+	+	++
Flavonoids	+	+	++

4.3 Biosynthesis of TiO₂

TiO₂ NPs have been successfully biosynthesized using the leaf extract of *Cassia alata* using the ultrasound-assisted method. After the biosynthesis process, the sol-gel treatment, ageing, washing of the precipitates of TiO₂, and drying process by using distilled water as the solvent, were carried out. Samples with different amounts of leaf extract (TiO₂-CA-2.5, TiO₂-CA-5.0, TiO₂-CA-7.5) showed a brown-coloured powder. The obtained powders of all samples with variations of colour due to the different amounts of leaf extract used are shown in Figure 2.

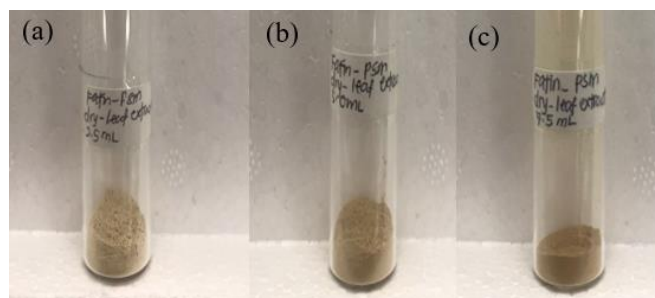


Figure 2. Images of (a) $\text{TiO}_2\text{-CA-2.5}$, (b) $\text{TiO}_2\text{-CA-5.0}$ (c) $\text{TiO}_2\text{-CA-7.5}$ samples before calcination.

After the calcination process, the colour of the samples changed to white due to the white pigment by the titania and the removal of the organic compound. The powdered samples after calcination are shown in Figure 3.

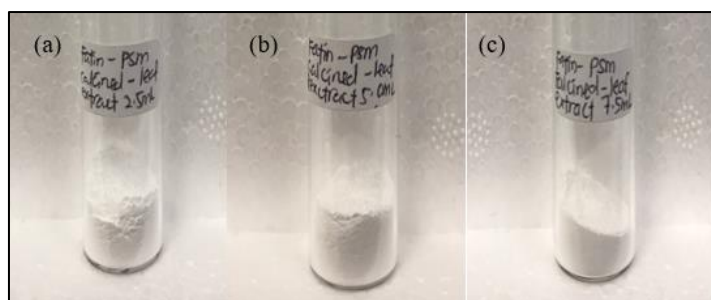


Figure 3. Images of (a) $\text{TiO}_2\text{-CA-2.5}$, (b) $\text{TiO}_2\text{-CA-5.0}$ (c) $\text{TiO}_2\text{-CA-7.5}$ samples after calcination.

4.4. Characterisations

4.4.1 FTIR spectroscopy analysis of *Cassia alata* leaf extract and TiO_2 NPs

The FTIR spectrum for the aqueous *Cassia alata* leaf extract is shown in Figure 4. From the spectrum, peaks at 3391 , 1605 , 1400 , 1077 and 671 cm^{-1} correspond to the OH band stretching of alcohols and phenolics, C=C aromatic ring stretching, nitro N–O bending, and the C–O vibrations of carboxylic acids and strong C=C bending, respectively.

Figure 4 shows the FTIR spectra obtained from the samples of the biosynthesized TiO_2 NPs. In the uncalcined samples (Figure 6a, c and e), wide absorption bands were observed at 3400 cm^{-1} and 1627 cm^{-1} due to the moisture absorption correspond to the O–H bond bending and stretching vibrations and Ti–OH band. The vibration bands at 1385 and 1056 cm^{-1} were assigned to the CO and C=C groups of aromatic. A broad absorption band in the region of 400 cm^{-1} - 800 cm^{-1} was also observed due to the Ti–O and Ti–O–O stretching vibrations in the samples of TiO_2 NPs. After that, the calcined samples (Fig 5 (b), (d), and (f)) showed a decrease in a wide absorption band due to the moisture at 3370 cm^{-1} and 1624 cm^{-1} . The calcined biosynthesized TiO_2 NPs with the condition of $500\text{ }^\circ\text{C}$ for 5 h indicate an absence of organic compounds' functional groups, which shows the complete calcination.

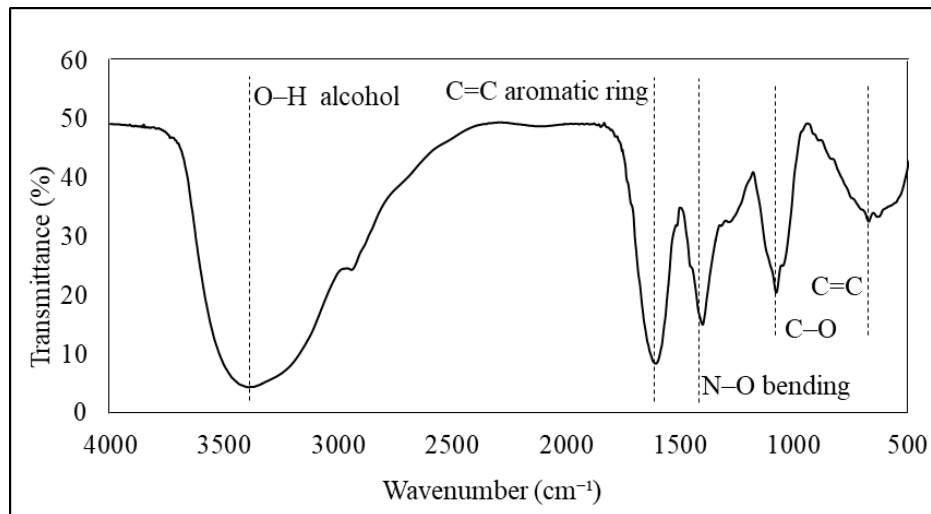


Figure 4. FTIR spectrum of aqueous *Cassia alata* leaf extract.

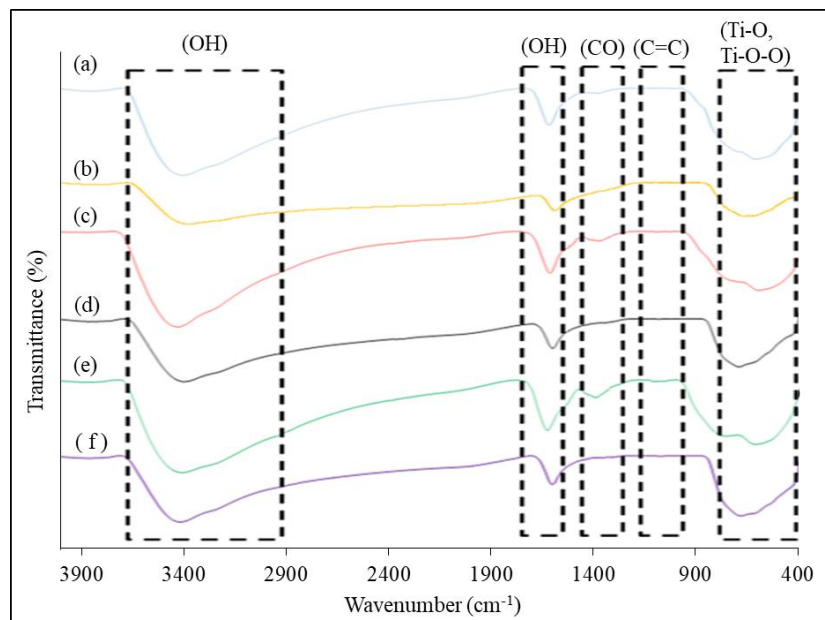


Figure 5. FTIR spectra of (a) dried $\text{TiO}_2\text{-CA-2.5}$, (b) calcined $\text{TiO}_2\text{-CA-2.5}$, (c) dried, $\text{TiO}_2\text{-CA-5.0}$, (d) calcined $\text{TiO}_2\text{-CA-5.0}$, (e) dried $\text{TiO}_2\text{-CA-7.5}$, and (f) calcined $\text{TiO}_2\text{-CA-7.5}$.

4.4.2 XRD Analysis of TiO_2 NPs

The crystallinity of the biosynthesized TiO_2 NPs was determined using XRD analysis. Figure 6 shows the XRD patterns of $\text{TiO}_2\text{-CA-2.5}$, $\text{TiO}_2\text{-CA-5.0}$ and $\text{TiO}_2\text{-CA-7.5}$ biosynthesized using different amounts of *Cassia alata* leaf extract. There are several major diffraction peaks that can be seen in the 2θ range of $20 - 80^\circ$, all assigned to the anatase phase. The major peaks were observed at 2θ values of 25.31 , 37.78 , 47.88 , 54.20 , 62.82 , 69.06 , and 75.13° corresponding to (101), (004), (200), (105), (204), (116), and (215) faces, respectively. All peaks are in good agreement with the standard spectrum (JCPDS no. 00-021-1272) which indicates the successful synthesis of TiO_2 NPs in the anatase phase.

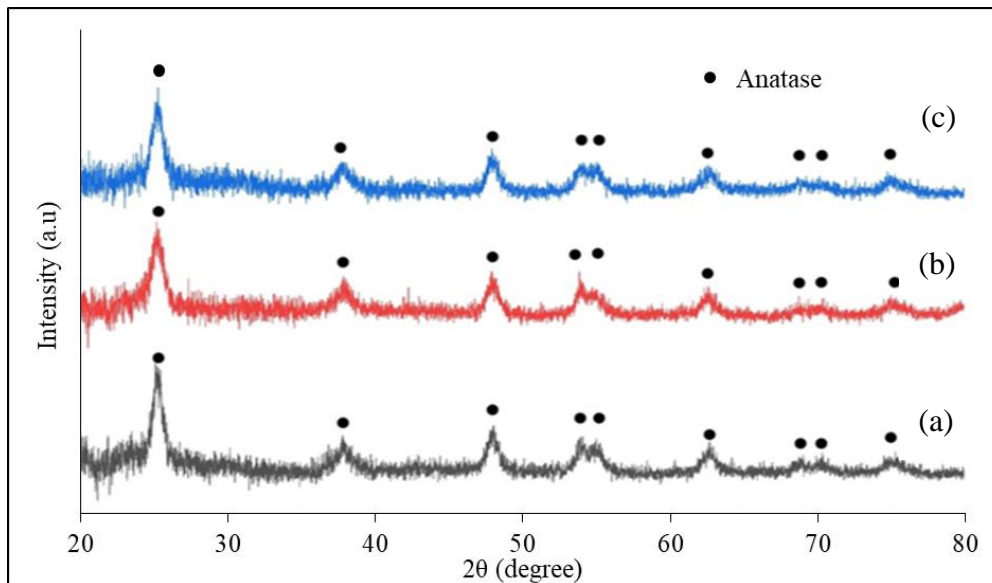


Figure 6. XRD patterns of the biosynthesized (a) $\text{TiO}_2\text{-CA-2.5}$, (b) $\text{TiO}_2\text{-CA-5.0}$ and (c) $\text{TiO}_2\text{-CA-7.5}$.

4.4.3 FESEM-EDX analysis of TiO_2 NPs

The morphology of the TiO_2 NPs synthesized from the leaf extract of *Cassia alata* can be seen in the FESEM images shown in Figure 7. From the images shown, the samples showed agglomeration, are non-uniform and almost spherical in shape. These results are in agreement with those obtained by [10]. The average particle sizes of $\text{TiO}_2\text{-CA-2.5}$, $\text{TiO}_2\text{-CA-5.0}$ and $\text{TiO}_2\text{-CA-7.5}$ were 22.85, 17.09, and 15.41 nm, respectively. This proved that TiO_2 particles in the nano-range have been successfully obtained. $\text{TiO}_2\text{-CA-7.5}$ gave a slightly smaller size of particles compared to the others. This most likely means that the surface area shown by this sample will also be the highest, as smaller particle size will usually result in a higher surface area [18].

The EDX analysis showed the presence of Ti and O peaks suggesting that the chemical composition has been successfully obtained. The weight percentage (w%) for each element in each sample is tabulated in Table 2.

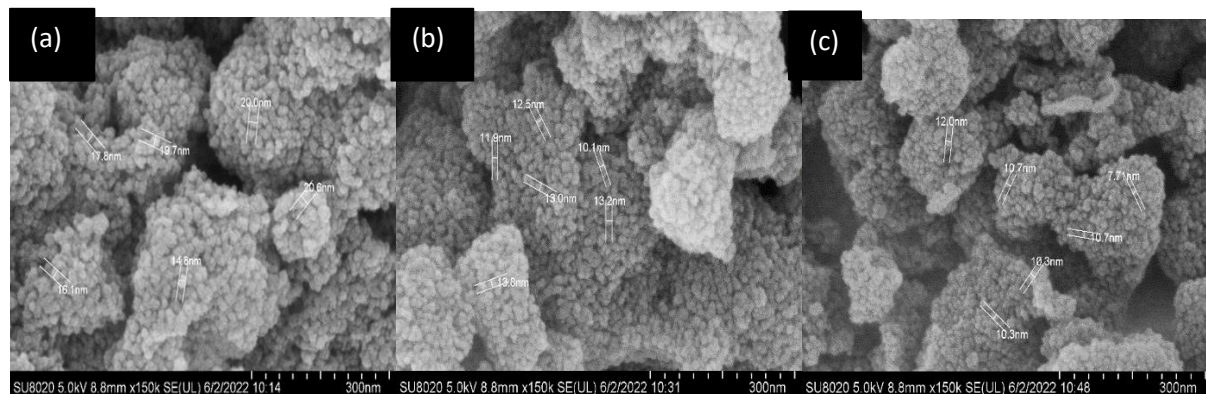


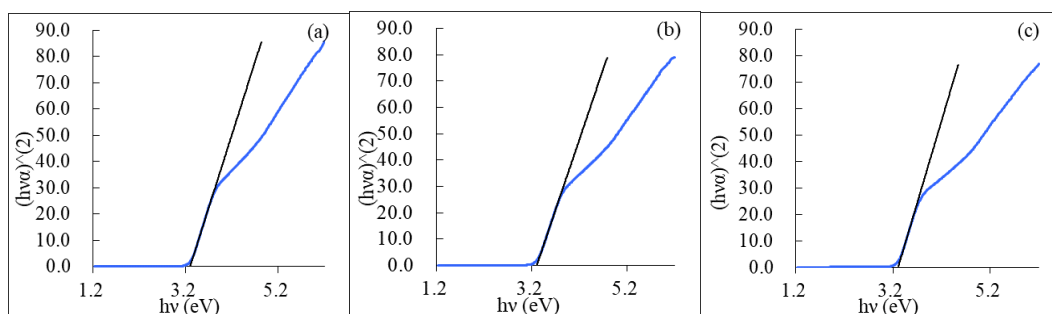
Figure 7. FESEM images of synthesized TiO_2 NPs from the leaf extract of *Cassia alata* with magnification of 10, 000 times; (a) $\text{TiO}_2\text{-CA-2.5}$, (b) $\text{TiO}_2\text{-CA-5.0}$, (c) $\text{TiO}_2\text{-CA-7.5}$

Table 2. EDX analysis of biosynthesized TiO₂-CA-2.5, TiO₂-CA-5.0 and TiO₂-CA-7.5

TiO ₂	Element	
	Ti (%)	O (%)
TiO ₂ -CA-2.5	58.8	41.2
TiO ₂ -CA-5.0	70.2	29.8
TiO ₂ -CA-7.5	54.5	45.5

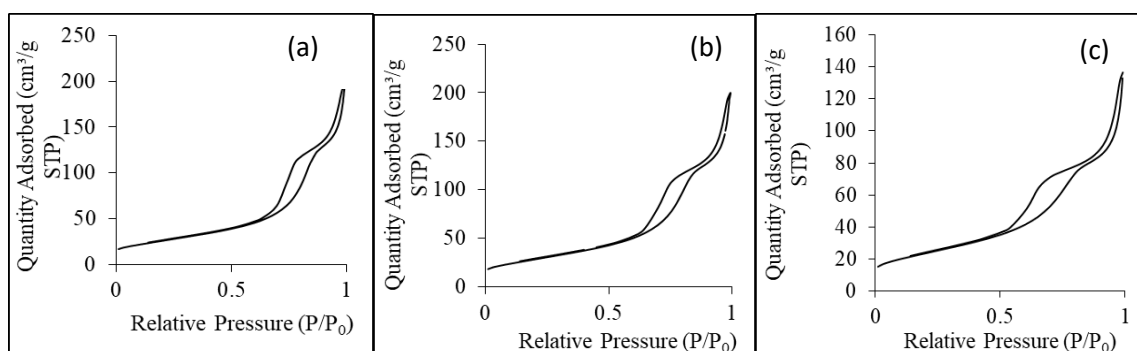
4.4.4 UV-Vis-NIR analysis of TiO₂ NPs

The bandgap energy was determined using the extrapolation of the UV-Vis-NIR absorption spectra. The value of the x-intercept was used to obtain the Tauc plot by plotting $(\alpha h\nu)^{1/2}$ vs $h\nu$. The bandgap energy value for each sample was obtained by linear extrapolating the plot, as shown in Figure 8. From the results obtained, a slight deviation from the actual anatase bandgap energy can be seen. Despite that, the prepared TiO₂ NPs were still in the acceptable range of the anatase phase [8].

**Figure 8.** Tauc plots of (a) TiO₂-CA-2.5, (b) TiO₂-CA-5.0 (c) TiO₂-CA-7.5

4.4.5 N₂ Adsorption-Desorption Analysis of TiO₂ NPs

The N₂ isotherms of the samples are shown in Figure 9. Type V isotherms were obtained for all the samples, which is characteristics of mesoporous materials, according to the IUPAC's classification [17]. The TiO₂-CA-2.5, TiO₂-CA-5.0, and TiO₂-CA-7.5 samples showed the H1 hysteresis loop type, which shows that these samples consist of well-defined cylindrical pore-channels.

**Figure 9.** N₂ adsorption-desorption isotherms of (a) TiO₂-CA-2.5, (b) TiO₂-CA-5.0, and (c) TiO₂-CA-7.5.

The pore size distribution of synthesized TiO₂ NPs was then obtained using the Barrett-Joyner-Halenda (BJH) method using the desorption branch plots. The average pore size distribution of TiO₂-CA-2.5 was 9.9449 nm. However, TiO₂-CA-5.0 gave a slightly smaller average pore size distribution which was 9.4221 nm and TiO₂-CA-7.5 gave the smallest value compared to others, which was 8.0293 nm. These results once again proved the mesoporosity of the samples. To summarise, by observing the isotherms of these 3 samples and their pore size distribution, it can be concluded that the samples are in the range of mesoporous size. From this result, TiO₂-CA-7.5 gave the smallest pore size distribution with a decrease in the volume of the pores and in the surface area.

The Brunauer-Emmett-Teller (BET) surface areas of samples and their pore volume were also measured and summarised in Table 3. From the data shown, the BET surface areas of TiO₂-CA- 5.0 was the largest compared to those of TiO₂-CA- 2.5 and TiO₂-CA- 7.5. As for the pore volume, TiO₂-CA-7.5 showed the smallest value among all three samples. Ideally, surface area should be inversely proportionate with the particle size, where a smaller particle size will result in a higher surface area [16]. However, based on the average particle size obtained from FESEM (Section 4.4.3), the smallest particle size was shown by TiO₂-CA- 7.5, which should have shown the highest surface area. Contrastly, this sample showed the lowest surface area based on the BET results. One possible explanation would be the non-uniformity of the samples. The particle size measured from FESEM might not represent the whole sample but only part of the samples. Hence, there could be more particles that were not measured but with different sizes. Although the sample with the smallest particle size gave the lowest BET surface area among all three samples, other factors also need to be taken into account as the performance photocatalytic activity of the sample does not rely solely only on the surface area.

Table 3. The BET surface area and pore volume of the biosynthesized TiO₂ NPs.

TiO ₂ NPs	S _{BET} (m ² /g)	Pore volume (cm ³ /g)
TiO ₂ -CA-2.5	94.4664	0.3048
TiO ₂ -CA-5.0	103.1434	0.3123
TiO ₂ -CA-7.5	84.4729	0.2144

4.4.6 Photocatalytic activity of TiO₂ NPs

The concentration of BPA used was 25 ppm and 4 types of samples, which were TiO₂-CA-2.5, TiO₂-CA-5.0 and TiO₂-CA-7.5 and commercial TiO₂, were used as the photocatalysts. From the result obtained as shown in Figure 10, after 60 minutes all the samples are capable to degrade the BPA solution under UV light irradiation but in different percentages. Out of the 3 biosynthesized TiO₂ NPs, the degradation percentage shown by sample TiO₂-CA-7.5 gave the highest value, which was 68.41% after 60 min. In fact, all 3 biosynthesized samples showed better photocatalytic activity as compared to commercial TiO₂, which only achieved 40.00% of BPA degradation only. The degradation percentages achieved by TiO₂-CA-2.5 and TiO₂-CA-5.0 samples were 47.62% and 57.14%, respectively.

Based on the results obtained from the characterizations and the photocatalytic test, it can be summarised that the biosynthesized TiO₂-CA-7.5, which was synthesized by using 7.5 mL of leaf extract, gave the best result in terms of physicochemical properties and photocatalytic activity. These superior results may most likely be due to the average small particle size shown by the sample. Photocatalytic performance relies on many factors, such as the average particle size, specific surface area, crystalline phase, crystal size, degree of crystallinity and crystal morphology [19]. From this work, TiO₂-CA-7.5 with a smaller particle size resulted in the highest photocatalytic performance. The result is in agreement with the findings reported by [20] where the anatase TiO₂ resulted in the best photocatalytic performance due to the small average of particle size.

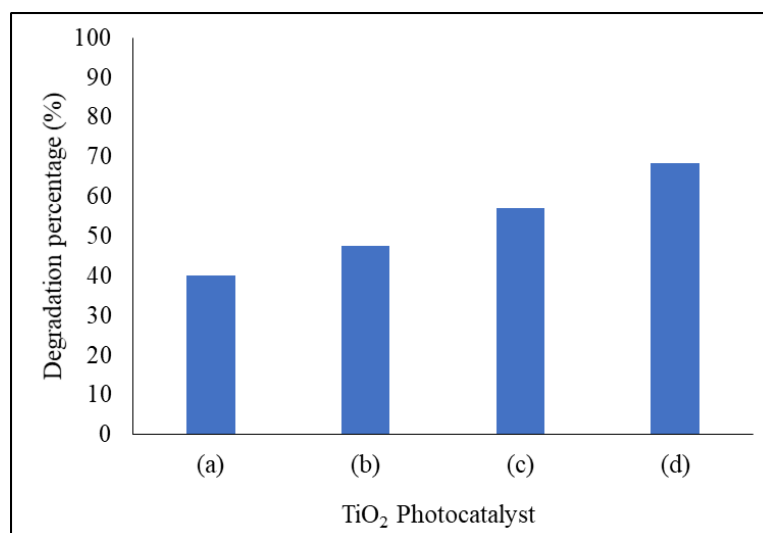


Figure 10. Degradation percentages of BPA solution under UV light irradiation in the presence of (a) commercial TiO₂, (b) TiO₂-CA-2.5, (c) TiO₂-CA-5.0 and (d) TiO₂-CA-7.5.

Conclusion

Based on the results of the characterization and photocatalytic activity testing obtained in this study, it can be deduced that using a higher amount of leaf extract will result in a smaller particle size obtained. The biosynthesized TiO₂ NPs with 7.5 mL of *Cassia alata* leaf extracts by using distilled water as the solvent is more efficient in producing TiO₂ NPs with good physicochemical properties and photocatalytic activity. Using the current method of utilising green natural resources in this study, the use of chemicals can be reduced, which are toxic to the environment and health.

Acknowledgement

The authors would like to acknowledge funding from the Ministry of Education (MOE), Malaysia, through Fundamental Research Grant Scheme (FRGS/1/2021/STG04/UTM/02/2) and Universitas Negeri Malang for the matching grant (R.J130000.7354.4B686 PY/2021/00490).

References

- [1] Ali, T., Tripathi, P., Azam, A., Raza, W., Ahmed, A. S., Ahmed, A., & Muneer, M. (2017). Photocatalytic performance of Fe-doped TiO₂ nanoparticles under visible-light irradiation. *Materials Research Express*, 4(1), 015022.
- [2] Zhu, D., & Zhou, Q. (2019). Action and mechanism of semiconductor photocatalysis on degradation of organic pollutants in water treatment: A review. *Environmental Nanotechnology, Monitoring & Management*, 12, 100255.
- [3] Soleimani, M., Ghasemi, J. B., & Badiei, A. (2021). Black Titania; Novel researches in Synthesis and Applications. *Inorganic Chemistry Communications*, 109092.
- [4] Riente, P., & Noël, T. (2019). Application of metal oxide semiconductors in light-driven organic transformations. *Catalysis Science & Technology*, 9(19), 5186-5232.
- [5] Mahato, M., Kim, J.-N., Tabassian, R., Rajabi-Abhari, A., Kim, J.-S., Nam, S., . . . Oh, I.-K. (2021). Mutually exclusive ytterbium and nitrogen co-doping of mesoporous titania-carbon for self-cleanable and sustainable triboelectric nanogenerators. *Nano Energy*, 90, 106615.
- [6] Rufai, Y., Chandren, S., & Basar, N. (2020). Influence of Solvents' Polarity on the Physicochemical Properties and Photocatalytic Activity of Titania Synthesized Using *Deinbollia pinnata* Leaves. *Frontiers in Chemistry*, 8, 1144.
- [7] Pham, D. Q., Pham, H. T., Han, J. W., Nguyen, T. H., Nguyen, H. T., Nguyen, T. D., . . . Vu, H. D. (2021). Extracts and metabolites derived from the leaves of *Cassia alata* L. exhibit in vitro and in vivo antimicrobial activities against fungal and bacterial plant pathogens. *Industrial Crops and Products*, 166, 113465.

- [8] Amanulla, A. M., & Sundaram, R. (2019). Green synthesis of TiO₂ nanoparticles using orange peel extract for anti-bacterial, cytotoxicity and humidity sensor applications. *Materials Today: Proceedings*, 8, 323-331.
- [9] Singh, J., Dutta, T., Kim, K.-H., Rawat, M., Samddar, P., & Kumar, P. (2018). 'Green'synthesis of metals and their oxide nanoparticles: applications for environmental remediation. *Journal of nanobiotechnology*, 16(1), 1-24.
- [10] Srinivasan, N. (2018). Pharmacognostical and phytochemical evaluation of *Cassia alata* Linn. *Journal of medicinal plants*, 6(5), 69-77.
- [11] Madkour, L. H. (2018). Ecofriendly green biosynthesised of metallic nanoparticles: bio-reduction mechanism, characterisation and pharmaceutical applications in biotechnology industry. *Global Drugs and Therapeutics*, 3(1).
- [12] Qamar, S. U. R., & Ahmad, J. N. (2021). Nanoparticles: Mechanism of biosynthesis using plant extracts, bacteria, fungi, and their applications. *Journal of Molecular Liquids*, 334, 116040.
- [13] Joseph, A., & Vijayanandan, A. (2021). Photocatalysts synthesised via plant mediated extracts for degradation of organic compounds: A review of formation mechanisms and application in wastewater treatment. *Sustainable Chemistry and Pharmacy*, 22, 100453.
- [14] Kumar, A., Khan, M., Zeng, X., & Lo, I. M. (2018). Development of g-C₃N₄/TiO₂/Fe₃O₄@ SiO₂ heterojunction via sol-gel route: a magnetically recyclable direct contact Z-scheme nanophotocatalyst for enhanced photocatalytic removal of ibuprofen from real sewage effluent under visible light. *Chemical Engineering Journal*, 353, 645-656.
- [15] Happy, A., Soumya, M., Kumar, S. V., Rajeshkumar, S., Sheba, R. D., Lakshmi, T., & Nallaswamy, V. D. (2019). Phyto-assisted synthesis of zinc oxide nanoparticles using *Cassia alata* and its anti-bacterial activity against *Escherichia coli*. *Biochemistry and biophysics reports*, 17, 208-211.
- [16] Singh, J., Dutta, T., Kim, K.-H., Rawat, M., Samddar, P., & Kumar, P. (2018). 'Green'synthesis of metals and their oxide nanoparticles: applications for environmental remediation. *Journal of nanobiotechnology*, 16(1), 1-24.
- [17] He, J., Du, Y. E., Bai, Y., An, J., Cai, X., Chen, Y., ... & Feng, Q. (2019). Facile formation of anatase/rutile TiO₂ nanocomposites with enhanced photocatalytic activity. *Molecules*, 24(16), 2996.
- [18] Phomma, S., Wutikhun, T., Kasamechonchung, P., Eksangsri, T., & Sapcharoenkun, C. (2020). Effect of calcination temperature on photocatalytic activity of synthesized TiO₂ nanoparticles via wet ball milling sol-gel method. *Applied Sciences*, 10(3), 993.
- [19] Marien, C. B., Marchal, C., Koch, A., Robert, D., & Drogui, P. (2017). Sol-gel synthesis of TiO₂ nanoparticles: effect of Pluronic P123 on particle's morphology and photocatalytic degradation of paraquat. *Environmental Science and Pollution Research*, 24(14), 12582-12588.
- [20] Zhang, J., Zhou, P., Liu, J., & Yu, J. (2014). New understanding of the difference of photocatalytic activity among anatase, rutile and brookite TiO₂. *Physical Chemistry Chemical Physics*, 16(38), 20382-20386